

1 **Comprehensive evaluation of *ACE2* expression in female ovary by single-cell RNA-seq**

2 **analysis**

3 Siming Kong<sup>a,c,d,f,h,l</sup>, Zhiqiang Yan<sup>a,c,d,l</sup>, Peng Yuan<sup>a,c,d</sup>, Xixi Liu<sup>a,c,d,e</sup>, Yidong Chen<sup>a,c,d,f,h</sup>,

4 Ming Yang<sup>a,c,d,f,h</sup>, Wei Chen<sup>a,c,d,f,h</sup>, Shi Song<sup>a,c,d</sup>, Jie Yan<sup>a,b,c,d,e,g</sup>, Liying Yan<sup>a,b,c,d,e,g,\*</sup>, Jie

5 Qiao<sup>a,b,c,d,e,f,g,h,\*\*</sup>

6

7 <sup>a</sup> Center for Reproductive Medicine, Department of Obstetrics and Gynecology, Peking

8 University Third Hospital, Beijing 100191, China;

9 <sup>b</sup> National Clinical Research Center for Obstetrics and Gynecology, Beijing 100191, China;

10 <sup>c</sup> Key Laboratory of Assisted Reproduction (Peking University), Ministry of Education,

11 Beijing 100191, China;

12 <sup>d</sup> Beijing Key Laboratory of Reproductive Endocrinology and Assisted Reproductive

13 Technology, Beijing 100191, China;

14 <sup>e</sup> Beijing Advanced Innovation Center for Genomics, Beijing 100871, China;

15 <sup>f</sup> Peking-Tsinghua Center for Life Sciences, Peking University, Beijing 100871, China;

16 <sup>g</sup> Research Units of Comprehensive Diagnosis and Treatment of Oocyte Maturation Arrest;

17 <sup>h</sup> Academy for Advanced Interdisciplinary Studies, Peking University, Beijing 100871, China.

18

19 \* Correspondence to: Liying Yan, Center for Reproductive Medicine, Department of

20 Obstetrics and Gynecology, Peking University Third Hospital, No. 49 North HuaYuan Road,

21 HaiDian District, Beijing 100191, China.

22 \*\* Correspondence to: Jie Qiao, Center for Reproductive Medicine, Department of Obstetrics

23 and Gynecology, Peking University Third Hospital, No. 49 North HuaYuan Road, HaiDian

24 District, Beijing 100191, China

25 E-mail addresses: [jie.qiao@263.net](mailto:jie.qiao@263.net) (J. Qiao), [yanliyingkind@aliyun.com](mailto:yanliyingkind@aliyun.com) (L. Y. Yan).

26 <sup>1</sup> Siming Kong and Zhiqiang Yan contributed equally to the work.

27

28 Abbreviations: SARS-CoV-2: severe acute respiratory coronavirus 2; SARS: Severe acute respiratory syndrome;

29 PGCs: primordial germ cells; ACE2: angiotensin-converting enzyme2; CatB/L: cathepsin B and L; scRNA-seq:

30 single-cell RNA-sequencing; COC: cumulus-oocyte complex.

31

## 32 **Abstract**

33 Pneumonia induced by severe acute respiratory coronavirus 2 (SARS-CoV-2) via ACE2

34 receptor may affect many organ systems like lung, heart and kidney. An autopsy report

35 revealed positive SARS-Cov-2 detection results in ovary, however, the

36 developmental-stage-specific and cell-type-specific risk in fetal primordial germ cells (PGCs)

37 and adult women ovary remained unclear. In this study, we used single-cell RNA-sequencing

38 (scRNA-seq) datasets spanning several developmental stages of ovary including PGCs and

39 cumulus-oocyte complex (COC) to investigate the potential risk of SARS-CoV-2 infection.

40 We found that PGCs and COC exhibited high *ACE2* expression. More importantly, the ratio

41 of *ACE2*-positive cells was sharply up-regulated in primary stage and *ACE2* was expressed in

42 all oocytes and cumulus cells in preovulatory stage, suggesting the possible risk of

43 SARS-CoV-2 infection in follicular development. CatB/L, not TMPRSS2, was identified to

44 prime for SARS-CoV-2 entry in follicle. Our findings provided insights into the potential risk

45 of SARS-CoV-2 infection during folliculogenesis in adulthood and the possible risk in fetal  
46 PGCs.

47

48 **Keywords:** SARS-CoV-2, *ACE2*, primordial germ cells, oocytes, cumulus-oocyte complex

49

## 50 **1. Introduction**

51 The outbreak of coronavirus disease 2019 caused by SARS-CoV-2 has been reported over  
52 22,000,000 cases of infections. Common symptoms of SARS-CoV-2 infected patients were  
53 fever, fatigue, dry cough, anorexia, and myalgia (Wang et al., 2020). The severe acute  
54 respiratory syndrome (SARS) infected binding receptor *ACE2* was also thought to be the  
55 receptor for SARS-CoV-2 as SARS-CoV-2 shared similar sequences in receptor-binding  
56 domain with SARS (Wan et al., 2020) and was confirmed to invade cells via *ACE2* by *in*  
57 *vitro* experiments (Zhou et al., 2020). Meanwhile, Hoffmann *et al* found that the serine  
58 protease *TMPRSS2* activity plays a crucial role in SARS-CoV-2 priming and endosomal  
59 cysteine proteases *CatB/L* may also have some effects in *TMPRSS2* negative cells (Hoffmann  
60 et al., 2020). Therefore, cells with *ACE2* and *TMPRSS2* expression and *TMPRSS2* negative  
61 cells with *ACE2* and *CatB/L* expression, may act as target cells and are susceptible to  
62 SARS-CoV-2 infection. Previous single-cell RNA-sequencing (scRNA-seq) analysis were  
63 mainly focused on the *ACE2* expression level of lung, heart, esophagus, kidney, bladder, and  
64 ileum (Zou et al., 2020). An autopsy report showed positive detection in ovary (W, 2020),  
65 however, the related details about patients such as specifically detective area, number of  
66 detective patients, ages were not included. As human ovary is a complex organ and contains

67 different types of cells, systematical *ACE2* expression analysis is critical in evaluation the  
68 risk in female ovary.

69 A key function of ovary is to generate fertilizable oocytes with full competence for  
70 reproduction (Oktem and Oktay, 2008). In female embryos, PGCs can form oocytes after  
71 controlled cell division and meiosis (Felici, 2005; Nikolic et al., 2016). In adult women,  
72 oocytes and cumulus cells in follicles plays a primary role in folliculogenesis (Zhang et al.,  
73 2018).

74 Different cell types may behave distinct susceptibility to SARS-CoV-2. We used our  
75 previous scRNA-seq data on PGCs (Li et al., 2017) and COC (Zhang et al., 2018) to  
76 construct a potential risk map of SARS-CoV-2 infection in fetal PGCs and adult women  
77 ovary.

78

## 79 **2. Results**

80

### 81 **2.1 Female PGCs exhibited high *ACE2* expression**

82

83 Female embryos form PGCs during development (FUJIMOTO et al., 1977; Saitou and  
84 Yamaji, 2012) and this process includes mitotic, RA signaling-responsive, meiotic, and  
85 oogenesis stages (Saitou and Yamaji, 2012). To evaluate the risk of SARS-CoV-2 infection in  
86 PGCs, we calculated developmental-stage-specific *ACE2* expression pattern in PGCs. *ACE2*  
87 expression were detected in all four cell types, including mitotic (3% *ACE2*-positive cells),  
88 RA signaling-responsive phase (10% *ACE2*-positive cells), meiotic prophase (10%

89 *ACE2*-positive cells), and oogenesis phase (59% *ACE2*-positive cells), with an increasing  
90 tendency in PGCs formation (Fig 1A, 1B). Previous study regarded cell types with >1%  
91 proportion of *ACE2*-positive cells as high risk of infection of SARS-CoV-2 (Zou et al., 2020),  
92 therefore, it suggested that PGCs may be at high risk of infection. To further study the  
93 potential risk of *ACE2*-positive PGCs, we compared the synchronization of *ACE2* and  
94 *TMPRSS2* expression. The results showed that *TMPRSS2* were nearly negatively expressed in  
95 PGCs, which revealed that *TMPRSS2* may not be used for cell entry by SARS-CoV-2 in  
96 PGCs (Fig 1C). We then evaluated the CatB/L expression in *ACE2* positive PGCs.  
97 Interestingly, we found that *CTSB* and *CTSL* displayed coincident expression with *ACE2*  
98 (Fig.S1A), indicating the possibility of SARS-CoV-2 priming by CatB/L in PGCs. In addition,  
99 somatic cells surrounding PGCs, including endothelial cells, early granulosa, mural granulosa,  
100 and late granulosa had no *ACE2* and *TMPRSS2* expression (Fig 1D-F). Although CatB/L was  
101 expressed in somatic cells surrounding PGCs (Fig.S1B), these somatic cells were still at low  
102 risk for SARS-CoV-2 infection. Taken together, PGCs may be at high risk while their  
103 surrounding somatic cells may be at low risk for SARS-CoV-2 infection.

104

## 105 **2.2 Oocytes and cumulus cells displayed high *ACE2* expression**

106

107 Female PGCs develop into immature oocytes in adult women ovary and the immature  
108 oocytes develop into mature oocytes through the primordial, primary, secondary, antral, and  
109 preovulatory stages (Zhang et al., 2018). To understand the developmental-stage-specific  
110 expression pattern of *ACE2* in oocytes and surrounding cumulus cells, we analyzed the *ACE2*

111 expression in folliculogenesis. We firstly calculated the proportion of *ACE2* expressed  
112 oocytes in different developmental stages during folliculogenesis. The results showed that  
113 *ACE2* were expressed in all five stages (primordial, primary, secondary, antral, and  
114 preovulatory follicles) with the least proportion of 52.9% *ACE2*-positive cells in primordial  
115 follicles and 100% *ACE2*-positive oocytes from antral to preovulatory stage (Fig 2A, 2B),  
116 reminding that oocytes during folliculogenesis may possibly be susceptible to virus infections.  
117 Moreover, the ratio of *ACE2*-positive cells was sharply up-regulated in primary follicles,  
118 indicating that *ACE2* may play a crucial role in this stage (Fig 2A, 2B). Intriguingly,  
119 *TMPRSS2* were also low-expressed while *CTSB* and *CTSL* were expressed in oocytes (Fig.  
120 2C, Fig.S2A), suggesting that CatB/L may also be primed for SARS-CoV-2 invasion. Taken  
121 together, oocytes during follicular development may be at high risk of SARS-CoV-2 infection,  
122 especially in antral and preovulatory stage.

123 To further understand the effects of *ACE2* on folliculogenesis, we performed Gene  
124 Ontology analysis between *ACE2*-positive and *ACE2*-negative oocytes in primary stage. We  
125 found that *ACE2* was involved in the regulation of autophagy and in key metabolic process,  
126 such as dephosphorylation, glycosylation, and amino acid transport (Fig.S3C).  
127 Meanwhile, we also tracked genes synchronously expressed with *ACE2* in folliculogenesis.  
128 Interestingly, we found that *USP13* had the same pattern with *ACE2* during follicular  
129 development (Fig.S3A). Likewise, GO analysis in down-regulated genes between  
130 *ACE2*-positive and *ACE2*-negative oocytes in primary stage also showed that *ACE2* was  
131 involved in cilium movement (Fig.S3C). Together, *ACE2* may be involved in metabolic  
132 process, regulation of autophagy and cilium movement during follicular activation and

133 ovulation.

134 Cumulus cells were neighboring cells of oocytes and may facilitate oocyte maturation  
135 (Chang et al., 2016). *ACE2* were expressed in cumulus cells of all five developmental stages,  
136 including primordial (12% *ACE2*-positive cells), primary (20% *ACE2*-positive cells),  
137 secondary (67% *ACE2*-positive cells), antral (92% *ACE2*-positive cells) and preovulatory  
138 (100% *ACE2*-positive cells) stages (Fig 2D, 2E), indicating that cumulus cells during  
139 folliculogenesis were at high risk of SARS-CoV-2 infection. To further confirm the  
140 SARS-CoV-2 entry, we also compared *TMPRSS2* and *ACE2* expression in cumulus cells. The  
141 results showed that there were hardly *TMPRSS2* positive cells in *ACE2* positive cells (Fig 2F).  
142 Interestingly, *CTSB* and *CTSL* were expressed in all stages during folliculogenesis (Fig.S2B)  
143 which meant that CatB/L may prime SARS-CoV-2 for cell entry. Together, cumulus cells  
144 during folliculogenesis may be at high risk for SARS-CoV-2 infection. Collectively, *ACE2*  
145 were high expressed in COC and SARS-CoV-2 may use CatB/L for priming.

146 To better study *ACE2* function in cumulus cells during follicle activation, we also  
147 performed Gene Ontology analysis in primary stage. The results showed that up-regulated  
148 genes in *ACE2*-positive cumulus cells were involved in the pattern recognition receptor  
149 signaling pathway, nucleobase-containing compound transport (Fig.S3D). Down-regulated  
150 genes in *ACE2* positive cumulus cells was involved in cilium assembly (Fig.S3D).  
151 Interestingly, down-regulated genes in *ACE2* positive oocytes were also related to cilium  
152 movement, suggesting that *ACE2* may have influences on cilium movement and cumulus  
153 cells may help with this process. Together, these results indicated that cumulus cells may help  
154 with the receptor recognition, compound transport and cilium movements during oocyte

155 maturation.

156

### 157 **3. Discussion**

158

159 Organs with *ACE2* expression may exhibit potential risk of SARS-CoV-2 infection and *ACE2*  
160 bound to SARS-CoV-2 S ectodomain presented 10-to 20-fold higher affinity than *ACE2*  
161 binding to SARS associated coronavirus (Wrapp et al., 2020). The SARS-Cov-2 positive  
162 detection results in female ovary reminded the infectious risk in female reproduction (W,  
163 2020). However, the developmental-stage-specific and cell-type-specific risk in fetal  
164 primordial germ cells (PGCs) and adult women ovary still needs investigation. In this study,  
165 we used scRNA-seq datasets from PGCs and COCs to systematically profile *ACE2*  
166 expression pattern in female ovary.

167 Our study first revealed that PGCs displayed high *ACE2* expression in all stages with 59%  
168 *ACE2* positive cells in oogenesis phase, indicating the high risk of SARS-CoV-2  
169 susceptibility in PGCs. And SARS-CoV-2 may use CatB/L to prime cell entry. However,  
170 whether SARS-CoV-2 can pass through the maternal-fetal barrier (Delorme-Axford et al.,  
171 2014) need more research.

172 We also found that *ACE2* were expressed in oocytes during folliculogenesis and all  
173 oocytes in antral and preovulatory stages were identified to express *ACE2*. *ACE2* were  
174 sharply up-regulated at the time of oocyte maturation in a rainbow trout study (Bobe et al.,  
175 2006). We also found that *ACE2* were expressed in cumulus cells especially in preovulatory  
176 stage (100% *ACE2*-positive cells). In addition, *ACE2* were hardly detected in mural granulosa

177 cells. It was consistent with that cumulus cells, not mural granulosa cells, in human  
178 preovulatory follicles showed high *ACE2* expression after 36 hours human chorionic  
179 gonadotropin administration (Grøndahl et al., 2012). Furthermore, our study found that  
180 CatB/L, rather than TMPRSS2, was identified to prime for SARS-CoV-2 entry in COC.

181 Besides, we found that the proportion of *ACE2*-positive cells was sharply up-regulated  
182 in oocytes at primary stage and *ACE2* may be related to metabolic process and regulation of  
183 autophagy. Autophagy involved USP13 (Xie et al., 2020) is synchronously expressed with  
184 *ACE2* during folliculogenesis. In addition, cumulus cells were also found to be related to  
185 receptor recognition and compound transport. These reminded us that *ACE2* changes may  
186 have influences on oocyte maturation.

187 Collectively, our study highlighted that the potential risk of SARS-CoV-2 infection in  
188 fetal PGCs and adult COCs with high *ACE2* expression. CatB/L may be used to prime  
189 SARS-CoV-2 infection. More experimental research and clinical observation were necessary  
190 to provide more robust evidence.

191

#### 192 **4. Materials and Methods**

193 We collected the published scRNA-seq datasets from different scales in ovary, including  
194 female PGCs (GSE86146) and COC (GSE107746). The data was processed according to the  
195 description in corresponding studies of each dataset (Li et al., 2017; Zhang et al., 2018). The  
196 expression level was log transformed in this analysis. The cells with *ACE2* expression>0  
197 were defined as *ACE2*-positive cells. According to the accepted consensus that lung AT2 cells  
198 are susceptible to SARS-CoV-2, the expression level of *ACE2* in AT2 cells were used as a

199 reference. Cell types with the *ACE2*-positive proportion >1% were regarded as high risk.  
200 Student t-test were used to identify differentially expressed genes between *ACE2*-positive and  
201 *ACE2*-negative cells in primary stage in COC. Gene Ontology analysis of the differentially  
202 expressed genes was performed using metasplice (Zhou et al., 2019).

203

#### 204 **Acknowledgements**

205 This work was supported by National Key Research and Development Program (2019YFA0801400,  
206 2018YFC1004000, 2017YFA0103801) and National Natural Science Foundation of China (81521002,  
207 81730038).

208

#### 209 **Data availability**

210 The datasets supporting the conclusions of this article are included in these published articles (Li et al.,  
211 2017; Zhang et al., 2018).

212

#### 213 **Compliance and ethics**

214 The authors declare that they have no competing interests.

215

#### 216 **References**

- 217 Bobe, J., Montfort, J., Nguyen, T., and Fostier, A. (2006). Identification of new participants in the rainbow trout  
218 (*Oncorhynchus mykiss*) oocyte maturation and ovulation processes using cDNA microarrays. *Reprod Biol*  
219 *Endocrinol* 4, 39.
- 220 Chang, H.M., Qiao, J., and Leung, P.C. (2016). Oocyte-somatic cell interactions in the human ovary-novel role of  
221 bone morphogenetic proteins and growth differentiation factors. *Hum Reprod Update* 23, 1-18.
- 222 Delorme-Axford, E., Sadovsky, Y., and Coyne, C.B. (2014). The Placenta as a Barrier to Viral Infections. *Annu Rev*  
223 *Viro* 1, 133-146.
- 224 Felici, M.D. (2005). Establishment of oocyte population in the fetal ovary: primordial germ cell proliferation and  
225 oocyte programmed cell death. *Reproductive BioMedicine Online* 10, 182-191.

226 FUJIMOTO, T., MIYAYAMA, Y., and FUYUTA, M. (1977). The origin, migration and fine morphology of human  
227 primordial germ cells. *The Anatomical Record*, 315-329.

228 Grøndahl, M.L., Andersen, C.Y., Bogstad, J., Borgbo, T., Hartvig Boujida, V., and Borup, R. (2012). Specific genes  
229 are selectively expressed between cumulus and granulosa cells from individual human pre-ovulatory follicles.  
230 *MHR: Basic science of reproductive medicine* 18, 572-584.

231 Hoffmann, M., Kleine-Weber, H., Schroeder, S., Kruger, N., Herrler, T., Erichsen, S., Schiergens, T.S., Herrler, G.,  
232 Wu, N.H., Nitsche, A., *et al.* (2020). SARS-CoV-2 Cell Entry Depends on ACE2 and TMPRSS2 and Is Blocked by a  
233 Clinically Proven Protease Inhibitor. *Cell*.

234 Li, L., Dong, J., Yan, L., Yong, J., Liu, X., Hu, Y., Fan, X., Wu, X., Guo, H., Wang, X., *et al.* (2017). Single-Cell  
235 RNA-Seq Analysis Maps Development of Human Germline Cells and Gonadal Niche Interactions. *Cell Stem Cell*  
236 20, 858-873 e854.

237 Nikolic, A., Volarevic, V., Armstrong, L., Lako, M., and Stojkovic, M. (2016). Primordial Germ Cells: Current  
238 Knowledge and Perspectives. *Stem Cells Int* 2016, 1741072.

239 Oktem, O., and Oktay, K. (2008). The ovary: anatomy and function throughout human life. *Ann N Y Acad Sci*  
240 1127, 1-9.

241 Saitou, M., and Yamaji, M. (2012). Primordial germ cells in mice. *Cold Spring Harb Perspect Biol* 4.

242 W, B.X. (2020). Autopsy of COVID-19 victims in China. *National Science Review*.

243 Wan, Y., Shang, J., Graham, R., Baric, R.S., and Li, F. (2020). Receptor recognition by the novel coronavirus from  
244 Wuhan: an analysis based on decade-long structural studies of SARS coronavirus. *Journal of virology*.

245 Wang, D., Hu, B., Hu, C., Zhu, F., Liu, X., Zhang, J., Wang, B., Xiang, H., Cheng, Z., Xiong, Y., *et al.* (2020). Clinical  
246 Characteristics of 138 Hospitalized Patients With 2019 Novel Coronavirus-Infected Pneumonia in Wuhan, China.  
247 *JAMA*.

248 Wrapp, D., Wang, N., Corbett, K.S., Goldsmith, J.A., Hsieh, C.-L., Abiona, O., Graham, B.S., and McLellan, J.S.  
249 (2020). Cryo-EM structure of the 2019-nCoV spike in the prefusion conformation. *Science*, 1260-1263.

250 Xie, W., Jin, S., Wu, Y., Xian, H., Tian, S., Liu, D.A., Guo, Z., and Cui, J. (2020). Auto-ubiquitination of NEDD4-1  
251 Recruits USP13 to Facilitate Autophagy through Deubiquitinating VPS34. *Cell Rep* 30, 2807-2819 e2804.

252 Zhang, Y., Yan, Z., Qin, Q., Nisenblat, V., Chang, H.M., Yu, Y., Wang, T., Lu, C., Yang, M., Yang, S., *et al.* (2018).  
253 Transcriptome Landscape of Human Folliculogenesis Reveals Oocyte and Granulosa Cell Interactions. *Mol Cell*  
254 72, 1021-1034 e1024.

255 Zhou, P., Yang, X.L., Wang, X.G., Hu, B., Zhang, L., Zhang, W., Si, H.R., Zhu, Y., Li, B., Huang, C.L., *et al.* (2020). A  
256 pneumonia outbreak associated with a new coronavirus of probable bat origin. *Nature* 579, 270-273.

257 Zhou, Y., Zhou, B., Pache, L., Chang, M., Khodabakhshi, A.H., Tanaseichuk, O., Benner, C., and Chanda, S.K.  
258 (2019). Metascape provides a biologist-oriented resource for the analysis of systems-level datasets. *Nat*  
259 *Commun* 10, 1523.

260 Zou, X., Chen, K., Zou, J., Han, P., Hao, J., and Han, Z. (2020). Single-cell RNA-seq data analysis on the receptor  
261 ACE2 expression reveals the potential risk of different human organs vulnerable to 2019-nCoV infection.  
262 *Frontiers of Medicine*, 1-8.

263

264

265 **Figure legends**

266 **Figure 1. The *ACE2* expression pattern in female PGCs and their surrounding somatic cells.**

267 A) Pie charts showed the ratio of *ACE2* expressed PGCs in each developmental stage. Mitotic, RA  
268 responsive, Meiotic, and Oogenesis represent four sequentially developmental stages of female PGCs.

269 B) Ratios of different *ACE2* expression level of PGCs in each developmental stage.

270 C) *ACE2* and *TMPRSS2* expression level of PGCs. Top: boxplots of *ACE2* and *TMPRSS2* expression  
271 level in each developmental stage. Bottom: heatmaps of *ACE2* and *TMPRSS2* expression level in each  
272 cell.

273 D) Pie charts showed the ratio of *ACE2* expressed PGC surrounding somatic cells. Endothelial:  
274 somatic cells surrounding the PGC in Mitotic stage; Early granulosa: somatic cells surrounding the  
275 PGC in RA responsive stage; Mural granulosa: somatic cells surrounding the PGC in Meiotic stage;  
276 Late granulosa: somatic cells surrounding the PGC in Oogenesis stage.

277 E) Ratios of different *ACE2* expression level of PGC surrounding somatic cells.

278 F) *ACE2* and *TMPRSS2* expression level of PGC surrounding somatic cells. Top: boxplots of *ACE2*  
279 and *TMPRSS2* expression level in PGCs surrounding somatic cells. Bottom: heatmaps of *ACE2* and  
280 *TMPRSS2* expression level in each cell.

281

282 **Figure 2. The *ACE2* expression pattern in COC during follicle development.**

283 A) Pie charts showed the ratio of *ACE2* expressed oocytes in COC of each developmental stage.  
284 Primordial, Primary, Secondary, Antral, and Preovulatory represent the five sequentially  
285 developmental stages of oocytes.

286 B) Ratios of different *ACE2* expression level of oocytes in COC of each developmental stage.

287 C) *ACE2* and *TMPRSS2* expression level of oocytes in COC. Top: boxplots of *ACE2* and *TMPRSS2*  
288 expression level in each developmental stage. Bottom: heatmaps of *ACE2* and *TMPRSS2* expression  
289 level in each cell.

290 D) Pie charts showed the ratio of *ACE2* expressed cumulus cells in COC of each developmental stage.  
291 Primordial, Primary, Secondary, Antral, and Preovulatory represent the five sequentially  
292 developmental stages of oocyte surrounding granulosa cells.

293 E) Ratios of different *ACE2* expression level of cumulus cells in COC of each developmental stage.

294 F) *ACE2* and *TMPRSS2* expression level of cumulus cells in COC. Top: boxplots of *ACE2* and  
295 *TMPRSS2* expression level in each developmental stage. Bottom: heatmaps of *ACE2* and *TMPRSS2*  
296 expression level in each cell.

297

298 **Fig.S1. *ACE2*, *CTSB* and *CTSL* expression in female embryo PGCs.**

299 A) *ACE2*, *CTSB* and *CTSL* expression level in PGCs. Top: boxplots of *ACE2*, *CTSB* and *CTSL*  
300 expression level in each developmental stage. Bottom: heatmaps of *ACE2*, *CTSB* and *CTSL*  
301 expression level in each cell.

302 B) *ACE2*, *CTSB* and *CTSL* expression level in PGCs surrounding somatic cells. Top: boxplots of  
303 *ACE2*, *CTSB* and *CTSL* expression level in PGCs surrounding somatic cells. Bottom: heatmaps of  
304 *ACE2*, *CTSB* and *CTSL* expression level in each cell.

305

306 **Fig.S2. *ACE2*, *CTSB* and *CTSL* expression in human COC during follicle development.**

307 A) *ACE2*, *CTSB* and *CTSL* expression level in oocytes. Top: boxplots of *ACE2*, *CTSB* and *CTSL*  
308 expression level in each developmental stage. Bottom: heatmaps of *ACE2*, *CTSB* and *CTSL*

309 expression level in each cell.

310 B) *ACE2*, *CTSB* and *CTSL* expression level in surrounding cumulus cells. Top: boxplots of *ACE2*,

311 *CTSB* and *CTSL* expression level in each developmental stage. Bottom: heatmaps of *ACE2*, *CTSB* and

312 *CTSL* expression level in each cell.

313

314 **Fig.S3. Gene Ontology analysis of genes between *ACE2*-positive and *ACE2*-negative cells**

315 A) Genes synchronously expressed with *ACE2* in oocytes.

316 B) Genes synchronously expressed with *ACE2* in cumulus cell.

317 C) Gene ontology terms of genes in oocytes between *ACE2*-positive and *ACE2*-negative cells in

318 primary stage. Top: gene ontology terms of up-regulated genes in oocytes. Bottom: gene ontology

319 terms of down-regulated genes in oocytes.

320 D) Gene ontology terms of genes in cumulus cells between *ACE2*-positive and *ACE2*-negative cells in

321 primary stage. Top: gene ontology terms of up-regulated genes in cumulus cells. Bottom: gene

322 ontology terms of down-regulated genes in cumulus cells.

Figure 1

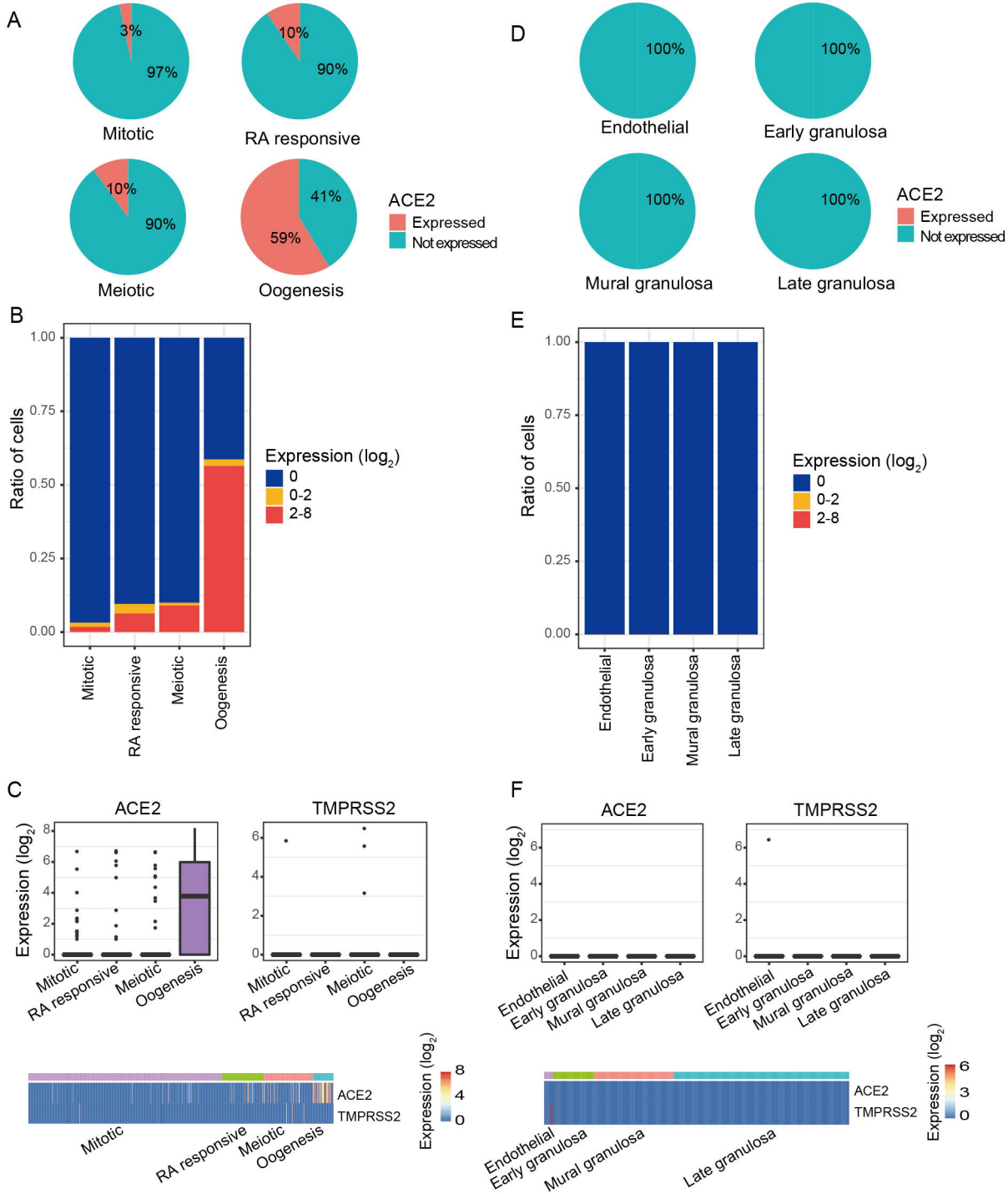


Figure 2

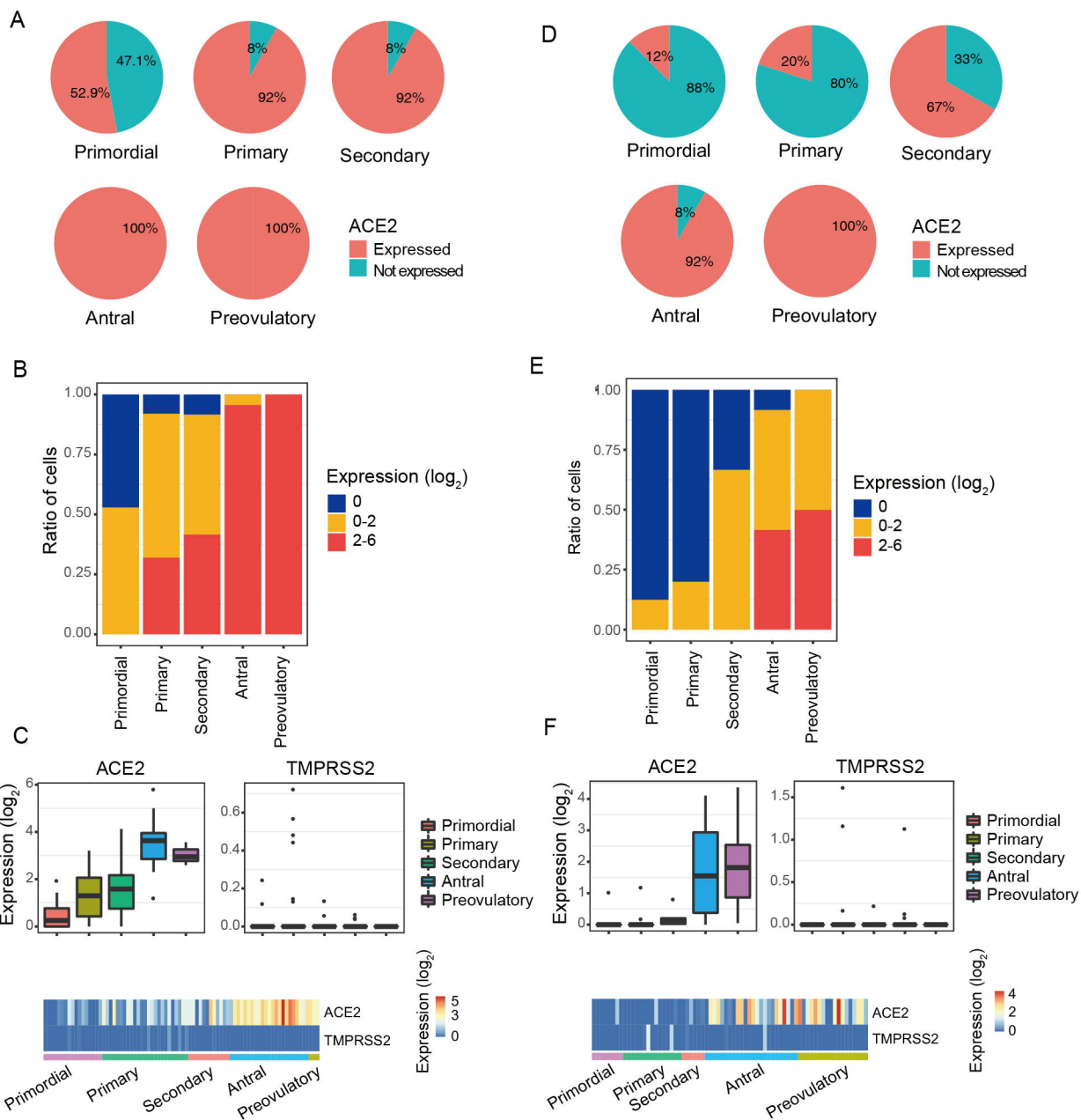
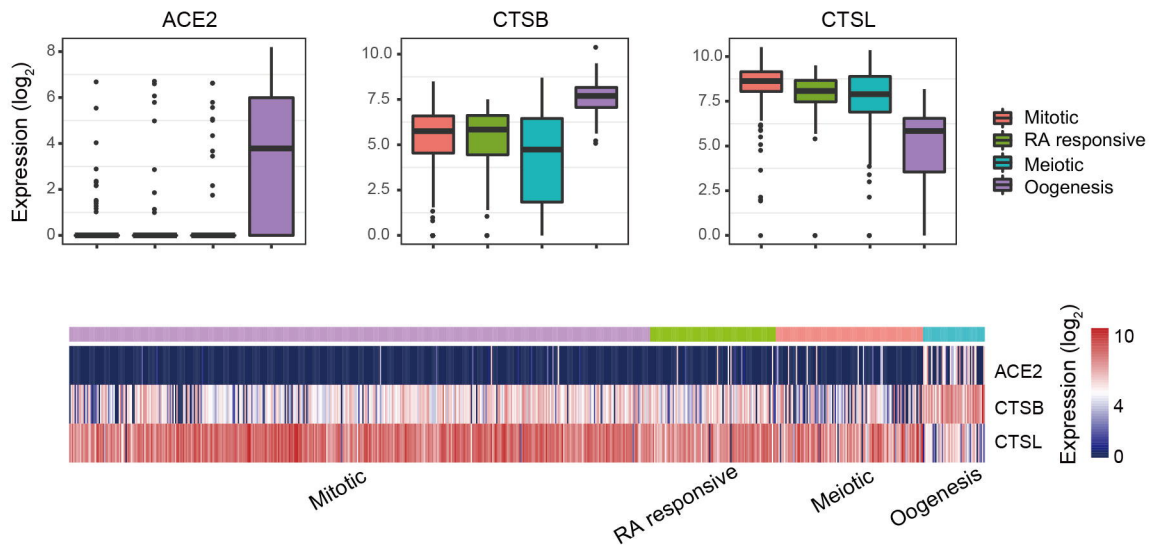


Figure S1

A



B

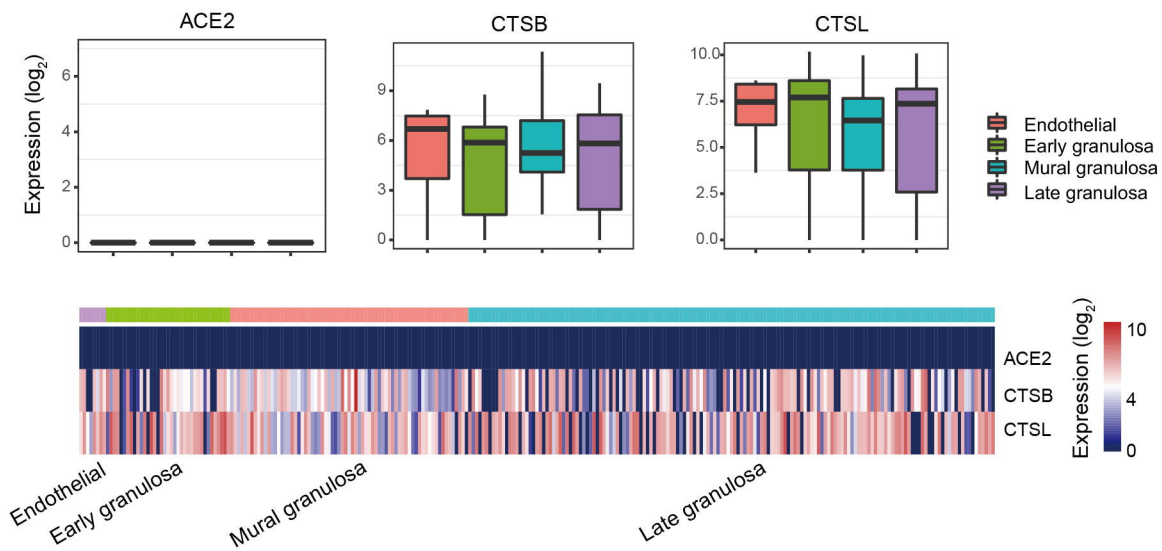


Figure S2

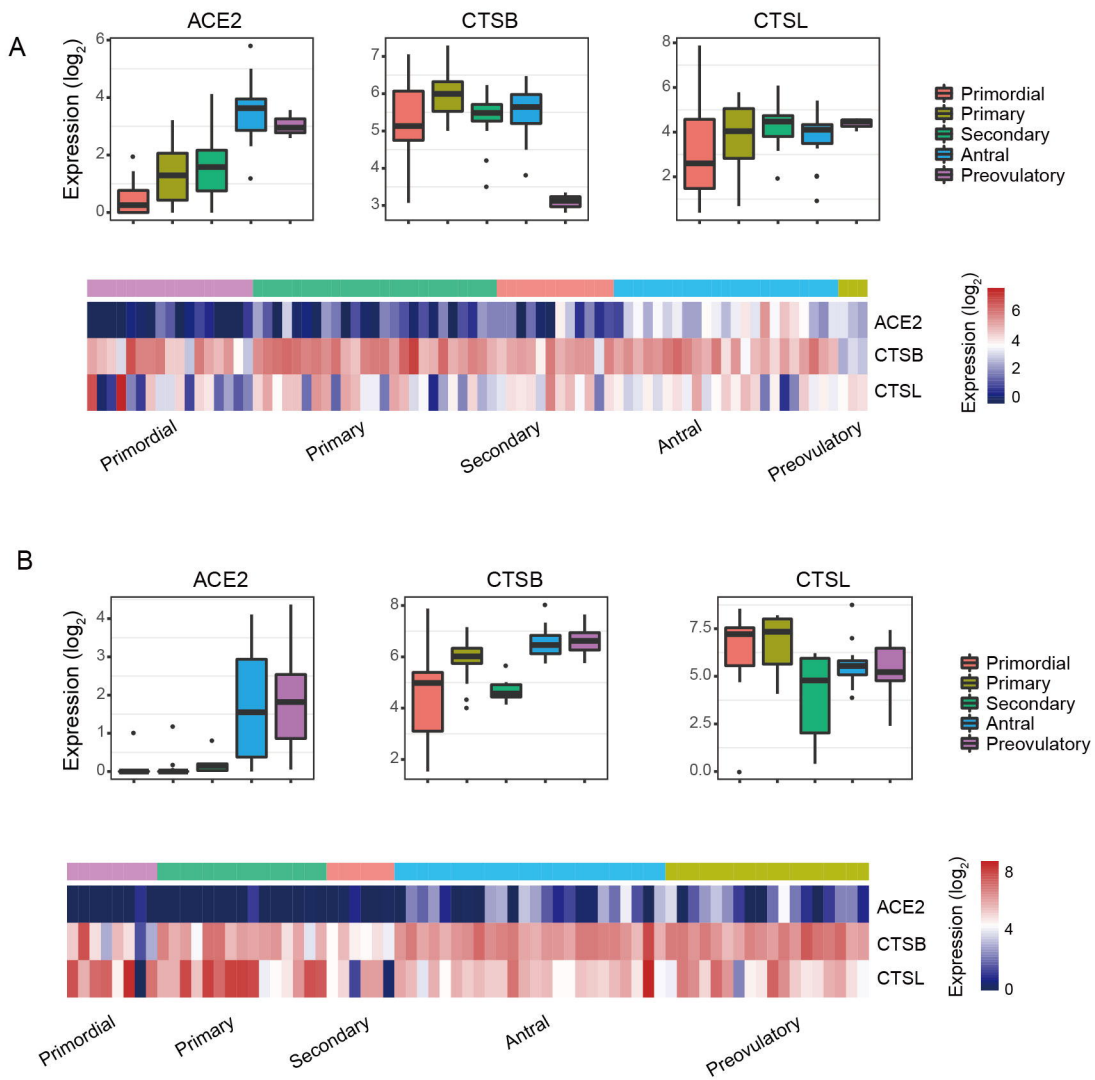
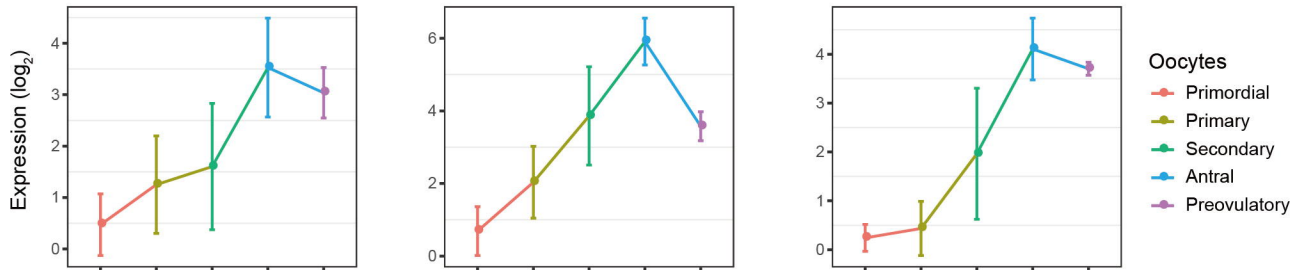


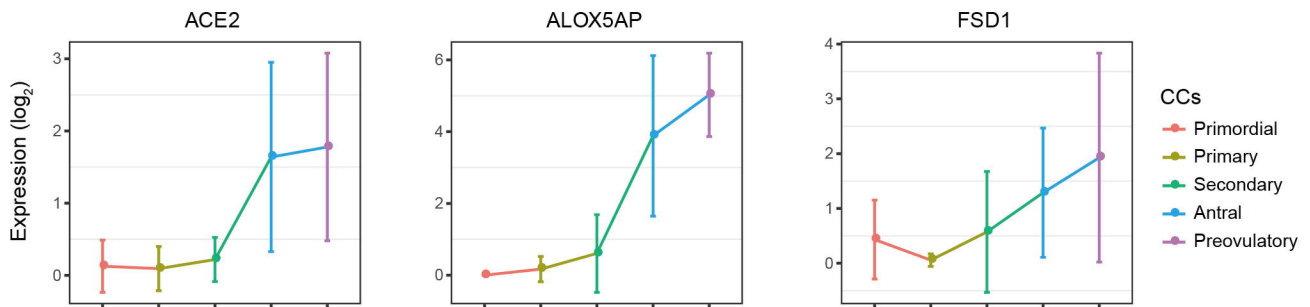
Figure S3

A

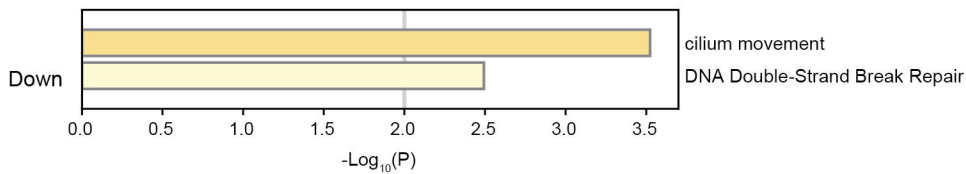
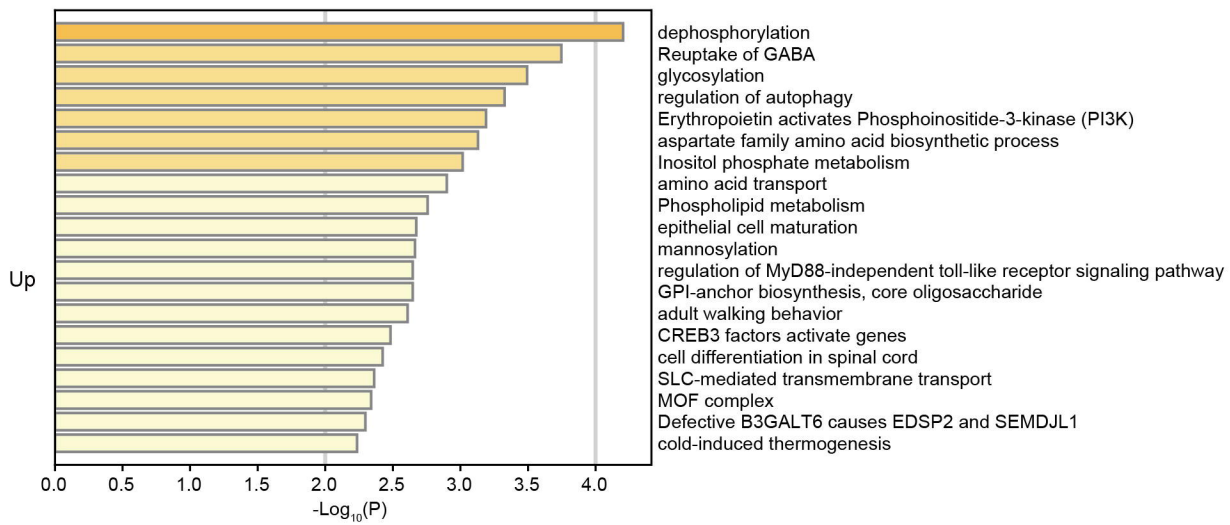
bioRxiv preprint doi: <https://doi.org/10.1101/2021.02.23.432460>; this version posted February 23, 2021. The copyright holder for this preprint (which was not certified by peer review) is the author/funder. All rights reserved. No reuse allowed without permission.



B



C



D

